# Fine structure of excitons in a quantum well in the presence of a nonhomogeneous magnetic field

J. A. K. Freire,* F. M. Peeters,† and A. Matulis‡
*Departement Natuurkunde, Universiteit Antwerpen (UIA), Universiteitsplein 1, B-2610 Antwerpen, Belgium*

V. N. Freire and G. A. Farias
*Departamento de Física, Universidade Federal do Ceará, Centro de Ciências Exatas, Campus do Pici, Caixa Postal 6030, 60455-760 Fortaleza, Ceará, Brazil*

(Received 24 March 2000)

The trapping of excitons in a semiconductor quantum well due to a circular symmetric nonhomogeneous magnetic field is studied. The effect of the spin state of the exciton on its trapping energy is analyzed, and the importance of the interaction of the orbital and spin Zeeman effect as compared to the diamagnetic term in the exciton Hamiltonian is emphasized. Magnetic-field profiles are considered, which can experimentally be created through the deposition of ferromagnetic disks on top of a semiconductor heterostructure. This setup gives rise to a magnetic dipole type of profile in the *xy* plane of the exciton motion. We find that the spin direction of the exciton influences its localization by changing the confinement region in the effective potential. The exciton confinement increases with magnetic-field intensity, and this is more pronounced when the exciton *g* factor is different from zero. The numerical calculations are performed for $GaAs/Al_xGa_{1-x}As$ quantum wells and we show that it open up a new realistic path for experiments designed to probe exciton trapping in semiconductors.

## I. INTRODUCTION

The trapping and guiding of atoms has been the subject of a number of experimental and theoretical works during the last few years.[1,2] Among the various methods that have been applied to the trapping of atoms, the magnetic one has been clearly recognized as the most powerful.[3,4] The possibility of exciton trapping in semiconductors has been actively pursued for many years.[5,6] Recently, nonhomogeneous stress was used in order to create an energy minimum for the trapping of excitons in GaAs quantum wells.[7] Several works have argued that the utilization of homogeneous magnetic fields during the trapping of excitons in semiconductors quantum wells will enhance Bose-Einstein effects in a gas of excitons.[8] In particular, Ref. 9 reported a strong increase of the exciton confinement properties above a critical threshold of uniform magnetic field. An alternative approach to localize excitons is by using nonhomogeneous magnetic fields. In a preceding paper,[10] we discussed the exciton lateral confinement in a GaAs two-dimensional electron gas (2DEG) in the presence of nonhomogeneous magnetic fields. We showed that excitons can be trapped in magnetic-field inhomogeneities, with a confinement degree that depends strongly on their angular momentum. Experimentally, nonhomogeneous magnetic fields were used to control the confinement of excitons in quantum wells, where spatially resolved photoluminescence (PL) and PL-excitation spectroscopy was utilized to measure the field gradient effect in the exciton lateral motion.[11]

With the continuing improvements in the experimental realization of spatially nonhomogeneous magnetic fields, several magnetic structures, which can be used for the trapping of particles, have been proposed,[12] such as: magnetic quantum dots produced by a scanning tunneling microscope lithographic technique,[13] magnetic superlattices created through the patterning of ferromagnetic materials integrated with semiconductors,[14] type-II superconducting materials deposited on conventional heterostructures,[15] and nonplanar 2DEG systems grown by molecular-beam epitaxy.[16] In particular, a magnetic dipole type of profile, which experimentally can be created by ferromagnetic materials deposited on top of semiconductor heterostructures, has attracted a great deal of interest.[10,17] This system is essentially different from the others since the local nonhomogeneous magnetic field has zero average magnetic-field strength. Furthermore, the magnetized disks can create much stronger magnetic-field inhomogeneities than the superconducting one.

In our previous paper,[10] we neglected the spin of the electron and the heavy hole and considered only their orbital motion. We showed that this could already induce a weak confinement of the excitons for special configurations of the nonhomogeneous magnetic-field profile. In the trapping of atoms, their spin/total angular momentum is the key quantity that leads to their confinement in a nonhomogeneous magnetic field. Therefore, we expect that in the case of excitons, the inclusion of the spin of the particles will lead to an increased confinement.

In this paper, we report on a detailed analysis of the trapping of excitons in a $GaAs/Al_xGa_{1-x}As$ quantum well in a nonhomogeneous magnetic field, taking into account spin effects. A magnetized disk deposited on top of a quantum well with a homogeneous magnetic field applied parallel to its growth direction *z*, i.e., perpendicular to the magnetic disk, generates the nonhomogeneous magnetic-field profile used in the present calculations. This system gives rise to a magnetic dipole type of profile in the *xy* plane of the exciton motion.[10,17,18] The effects of the well confinement and the importance of the orbital and spin Zeeman splitting, and the diamagnetic contributions to the exciton trapping energy and the wave function are analyzed.

 

The paper is organized as follows. In Sec. II the theoretical procedure used to obtain the exciton Hamiltonian in a quantum well in nonhomogeneous magnetic fields is given. The circular magnetic trap used in this paper is also presented in Sec. II. The calculation method to obtain the exciton trapping energy, the exciton effective mass and its effective confinement potential are discussed in Sec. III. Our numerical results for GaAs/$Al_xGa_{1-x}$As quantum wells are presented and discussed in Sec. IV. These theoretical results strongly suggest that it is possible to realize experimentally exciton trapping using nonhomogeneous magnetic fields. Our results are summarized in Sec. V.

## II. THEORETICAL MODEL

### A. Exciton Hamiltonian

The exciton Hamiltonian describing the electron and heavy-hole motion in a quantum well in nonhomogeneous magnetic fields can be written as follows:

$$H=H^{2D}(\mathbf{r}_e,\mathbf{r}_h)+W(r,z_{e,h})+H^{\perp}(z_{e,h})+H^{m_z}(\mathbf{r}_e,\mathbf{r}_h), \tag{1}$$

where

$$H^{2D}(\mathbf{r}_e,\mathbf{r}_h)=\frac{\hbar^2}{2m^*_{e,\|}}\left\{-i\nabla^{2D}_e+\frac{e}{\hbar c}\mathbf{A}(\mathbf{r}_e)\right\}^2 + \frac{\hbar^2}{2m^*_{h,\|}}\left\{-i\nabla^{2D}_h-\frac{e}{\hbar c}\mathbf{A}(\mathbf{r}_h)\right\}^2-\frac{\gamma e^2}{\varepsilon r}, \tag{2a}$$

$$W(r,z_{e,h})=\frac{\gamma e^2}{\varepsilon r}-\frac{e^2}{\varepsilon\sqrt{r^2+(z_e-z_h)^2}}, \tag{2b}$$

$$H^{\perp}(z_{e,h})=-\frac{\hbar^2}{2m^*_{e,\perp}}\frac{\partial^2}{\partial z_e^2}+V_e(z_e)-\frac{\hbar^2}{2m^*_{h,\perp}}\frac{\partial^2}{\partial z_h^2}+V_h(z_h), \tag{2c}$$

$$H^{m_z}(\mathbf{r}_e,\mathbf{r}_h)=\mu_B\sum_{i=x,y,z}g_{e,i}S_{e,i}B_i(\mathbf{r}_e) - 2\mu_B\sum_{i=x,y,z}(k_iJ_{h,i}+q_iJ^3_{h,i})B_i(\mathbf{r}_h) - \frac{2}{3}\sum_{i=x,y,z}c_iS_{e,i}J_{h,i}. \tag{2d}$$

The in-plane Hamiltonian $[H^{2D}(\mathbf{r}_e,\mathbf{r}_h)]$ describes the electron and hole motion in the $xy$ plane in a nonhomogeneous magnetic field, which is represented by the vector potential $\mathbf{A}(\mathbf{r})$. We will make use of a variational approach[19] to assume that the difference between the 2D and 3D Coulomb interactions $[W(r,z_{e,h})]$ can be made very small by the choice of an optimum value for $\gamma$,[20] which is a variational parameter that is calculated from the average of $W(r,z_{e,h})$ over the exciton wave function. The perpendicular contribution $[H^{\perp}(z_{e,h})]$ describes the exciton confinement in the quantum well, i.e., in the $z$ direction, which is not affected by the magnetic field. The exciton spin interaction with the magnetic field is described by the spin Hamiltonian $[H^{m_z}(\mathbf{r})]$. The terms in the latter correspond to the electron and heavy-hole Zeeman spin interaction, and to the spin-spin coupling energy, respectively.[21]

In Eq. (2), $m^*_{e,\perp}$, $m^*_{h,\perp}$ ($m^*_{e,\|}$, $m^*_{h,\|}$) are the perpendicular (in-plane) electron and heavy-hole effective masses, $S_{e,i}$ and $J_{h,i}$ ($g_{e,i}$ and $k_i$, $q_i$) are related to the electron and heavy-hole spin (Luttinger-Zeeman splitting constants), respectively, $m_z=S_{e,i}+J_{h,i}=\pm1,\pm2$, is the total spin angular momentum, $\mu_B=e\hbar/2m^*_{e,\|}c$ is the Bohr magneton, and $c_i$ is the spin-spin coupling constant related to the zero-field spin interaction. We will assume an isotropic dispersion for electrons and holes. Notice that $\mathbf{r}_e$, $\mathbf{r}_h$ are 2D coordinates and give the $xy$ plane position of the electron and hole, respectively.

To simplify the in-plane $[H^{2D}(\mathbf{r}_e,\mathbf{r}_h)]$ and spin $[H^{m_z}(\mathbf{r}_e,\mathbf{r}_h)]$ Hamiltonian, we introduce the exciton relative and center-of mass coordinates, $\mathbf{r}=\mathbf{r}_e-\mathbf{r}_h$, and $\mathbf{R}=(m^*_e\mathbf{r}_e+m^*_h\mathbf{r}_h)/M$, respectively, with $M=(m^*_e+m^*_h)$ the exciton mass. Following Ref. 10, we apply the adiabatic approach[22] in which we assume that the exciton relative motion is fast as compared to the center-of-mass motion. Following the approach of Freire *et al.*,[10] the $H^{2D}(\mathbf{r}_e,\mathbf{r}_h)$ Hamiltonian can be separated in a center-of-mass and a relative Hamiltonian, i.e., $H^{2D}(\mathbf{r}_e,\mathbf{r}_h)=H^{CM}(\mathbf{R})+H^r_\gamma(\mathbf{r},\mathbf{R},\nabla_R)$, with $H^{CM}(\mathbf{R})=-(\hbar^2/2M)\nabla^2_R$, and

$$H^r_\gamma(\mathbf{r},\mathbf{R},\nabla_R)=-\frac{\hbar^2}{2\mu}\nabla^2_r-\frac{\gamma e^2}{\varepsilon r}+W_1+W_2, \tag{3}$$

where $W_1=(e/2\mu c)\xi\mathbf{B}(\mathbf{R})\cdot\mathbf{L}+(ie\hbar/2Mc)[\mathbf{B}(\mathbf{R})\times\nabla_R-\nabla_R\times\mathbf{B}(\mathbf{R})]\cdot\mathbf{r}$ and $W_2=(e^2/8\mu c^2)B(\mathbf{R})^2r^2$ are terms related with the first and the second power in the magnetic-field strength, respectively.[10] In the above Hamiltonian, $\mu=m^*_em^*_h/M$ is the exciton reduced mass, $\xi=(m^*_h-m^*_e)/M$, and $\mathbf{L}=\mathbf{r}\times(-i\hbar\nabla_r)$ is the exciton angular momentum associated to the relative motion.

In the adiabatic approximation, the magnetic field in the spin Hamiltonian [see $H^{m_z}(\mathbf{r}_e,\mathbf{r}_h)$ in Eq. (2d)] can be expanded to zero order in the relative coordinates, i.e., $\mathbf{B}(\mathbf{r}_{e,h})=\mathbf{B}(\mathbf{R})$. With this assumption, the exciton spin Hamiltonian can be written as:

$$H^{m_z}(\mathbf{R})=\mu_B\sum_{i=1}^{3}\left[g_{e,i}S_{e,i}-\frac{1}{3}g_{h,i}J_{h,i}\right]B_i(\mathbf{R}) - \frac{2}{3}\sum_{i=1}^{3}c_iS_{e,i}J_{h,i}, \tag{4}$$

where we introduced the following definitions for the exciton heavy-hole $g$ factor $g_{h,x}=3q_x$, $g_{h,y}=-3q_y$, and $g_{h,z}=6k_z+13.5q_z$.[21]

Following the adiabatic approach, the total exciton wave function can be written as $\Psi^{m_z}(\mathbf{R},\mathbf{r},z_{e,h})=\Phi(\mathbf{r})\psi(\mathbf{R})F(z_{e,h})\mathcal{L}^{m_z}(\mathbf{R})$, where $\Phi(\mathbf{r})$ [$\psi(\mathbf{R})$] is the exciton wave function associated to the relative (center-of-mass) motion, and $\mathcal{L}^{m_z}(\mathbf{R})$, $F(z_{e,h})$ is the exciton wave function corresponding to the spin and to the confinement in the quantum well, respectively. Please notice that in the case of the exciton motion in a homogeneous magnetic field, the

spin interaction with the magnetic field can be solved separately from the center-of-mass and relative motion coordinates. Therefore, we assume here that there is no coupling between the wave function related to the exciton spin contribution and those of the exciton center-of-mass and relative motion. Finally, we obtain the following Schrödinger equations:

$$\{H^{CM}(\mathbf{R})+E^{r}(\gamma,\mathbf{R},\nabla_R)+E^{m_z}(\mathbf{R})+E^{\perp}-E\}\psi(\mathbf{R})=0, \tag{5a}$$

$$\{H^{r}_{\gamma}(\mathbf{r},\mathbf{R},\nabla_R)-E^{r}(\gamma,\mathbf{R},\nabla_R)\}\Phi(\mathbf{r})=0, \tag{5b}$$

$$\{H^{m_z}(\mathbf{R})-E^{m_z}(\mathbf{R})\}\mathcal{L}^{m_z}(\mathbf{R})=0, \tag{5c}$$

$$\{H^{\perp}(z_{e,h})-E^{\perp}\}F(z_{e,h})=0. \tag{5d}$$

The variational parameter ($\gamma$) is chosen in such a way to minimize the expectation value of $W(r,z_{e,h})$. The optimum condition is found when

$$\triangle E'=\langle\Phi(\mathbf{r})F(z_{e,h})|W(r,z_{e,h})|\Phi(\mathbf{r})F(z_{e,h})\rangle=0. \tag{6}$$

The above equation determines $\gamma_{\min}$, which is inserted into the exciton relative motion energy $E^{r}(\gamma,\mathbf{R},\nabla_R)$.

### B. The nonhomogeneous magnetic field

Here, we are interested in the possibility of exciton trapping by using a confinement potential that is created by a circular nonhomogeneous magnetic field. Experimentally, these magnetic-field profiles can, e.g., be created by the deposition of nanostructured ferromagnetic disks (or superconducting disks) on top of a semiconductor heterostructure with a homogeneous magnetic field applied perpendicular to the $xy$ plane. This produces a nonhomogeneous perpendicular magnetic field in the plane.[17,18] In this paper, we consider a magnetized disk on top of a GaAs/$Al_xGa_{1-x}$As quantum well, which creates a magnetic dipole type of profile. A sketch of the experimental setup is shown in Fig. 1(a). This nonhomogeneous magnetic-field profile is for $h \ll a$ given by the following equation:[10]

$$\begin{aligned}B_z(R)=B_a+2B_0^D\frac{a(a+R)}{R\sqrt{(a+R)^2+d^2}}&\\ \times\left\{-E(p^2)+\left(1-\frac{p^2}{2}\right)K(p^2)\right\}&\\ +B_0^D\frac{a(a^2-R^2+d^2)}{R^2\sqrt{aR}}p^3&\\ \times\left\{-\frac{\partial}{\partial p^2}E(p^2)-\frac{1}{2}K(p^2)\right.&\\ \left.+\left(1-\frac{p^2}{2}\right)\frac{\partial}{\partial p^2}K(p^2)\right\},&\end{aligned} \tag{7}$$

where $p=2\sqrt{aR}/\sqrt{(a+R)^2+d^2}$, $B_0^D=h\mathcal{M}/a$ is the strength of the magnetization of the disk, $B_a$ is the uniform applied field, $h$ is the disk thickness, $a$ is the disk radius, $d$ is the distance of the magnetic disk to the middle of the quantum well, $\mathcal{M}$ is the magnetization (in units of $\mu_0\mathcal{M}/4\pi$, where $\mu_0$ is the permeability of free space), $R$ is the radial coordinate in the $xy$ plane, and $K(x)$ [$E(x)$] is the elliptic integral of first (second) type. The magnetic-field profile $B_z(R)$ is shown in Fig. 1(b), for $a=2$ $\mu$m, $d=0.2$ $\mu$m, $B_0^D=0.05$ T, and for different values of the external applied magnetic field $B_a=0$, $-0.25$ T, and 0.35 T. Notice that for this magnetic-field profile, the average magnetic-field strength is zero, which give us the additional possibility to apply a background field $B_a$ to shift this magnetic-field profile up and down. We will show that this results into two different effective confinement profiles for the exciton.

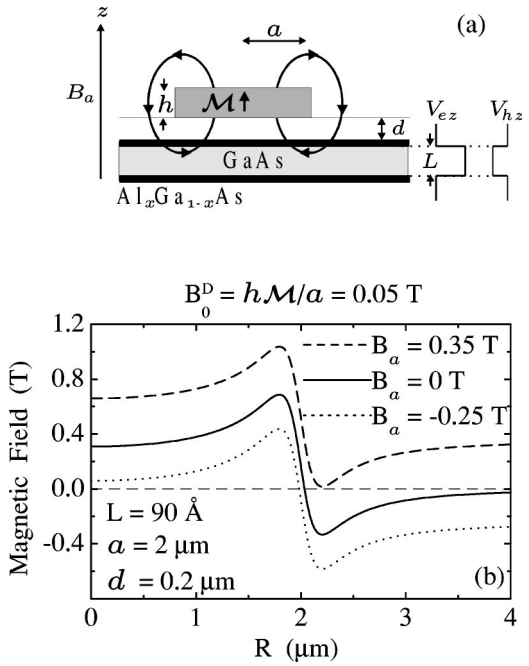


FIG. 1. (a) Experimental setup to create a magnetic dipole type of profile in the $xy$ plane of the exciton motion in a quantum well. Here $a$ ($h$) is the disk radius (thickness), $d$ is the distance of the disk to the middle of the quantum well, $\mathcal{M}$ the magnetization, $B_a$ is an uniform applied field, and $B_0^D$ is the strength of the disk magnetization. (b) The magnetic dipole type of profile as a function of the radial coordinate $R$ for different values of the background magnetic field.

## III. EFFECTIVE MASS AND CONFINEMENT POTENTIAL

In order to estimate the exciton confinement, we defined the trapping energy $E_T$ as the energy difference between an excitonic state in the homogeneous applied field $B_a$ and the corresponding state in the nonhomogeneous magnetic field:

$$E_T=E^{r}(\gamma,B_a)+E^{m_z}(B_a)+E^{\perp}-E. \tag{8}$$

Thus, the important terms (effective potentials) which determine $E_T$ in Eq. (5a) are only those appearing in Eqs. (5b)–(5d) which are $B(R)$ dependent. Therefore, the Hamiltonian corresponding to the exciton confinement in the quantum well does not have to be solved in order to obtain the trapping energy. Indeed the corresponding result will cancel out in the $E_T$ calculation. All the well confinement related contribution to the exciton trapping is then determined through the $\gamma$ parameter [see Eqs. (5b) and (6)]. It is worthwhile to

point out that if we are interested in calculating the exciton binding energy, all these terms [Eqs. (5b)–(5d)] have to be included.

Following Ref. 10, the exciton relative motion [see Eq. (5b)] can be solved by perturbation techniques, where all the $B(R)$-dependent terms are treated as perturbations. The corresponding eigenvalues are

$$E^r(\gamma,R,\nabla_R)=\frac{e\hbar}{2\mu c}\xi m_r B_z(R)+\frac{e^2}{8\mu c^2}\beta_{m_r}^{n_r}\gamma^{-2}B_z(R)^2 + \frac{e^2\mu}{2M^2c^2}\alpha_{m_r}^{n_r}\gamma^{-4}\nabla_R[B_z(R)^2\nabla_R], \tag{9}$$

with the following wave function:

$$\Phi_0^{n_r,m_r}(\mathbf{r})=A_{n_r,m_r}\left(\frac{2\gamma r}{a_B^*(n_r-1/2)}\right)^{|m_r|} \times\exp\left(im_r\varphi-\frac{\gamma r}{a_B^*(n_r-1/2)}\right) \times L_{n_r+|m_r|-1}^{2|m_r|}\left(\frac{2\gamma r}{a_B^*(n_r-1/2)}\right), \tag{10}$$

where $n_r$, $m_r$ are quantum numbers of the exciton relative motion, $a_B^*=\varepsilon\hbar^2/\mu e^2$ is the effective Bohr radius, $A_{n_r,m_r}$ is the normalization constant, $L_n^{(\alpha)}(x)$ is the generalized Laguerre polynomial, and $\alpha_{m_r}^{n_r}$ and $\beta_{m_r}^{n_r}$ (in units of $a_B^{*4}$ and $a_B^{*2}$, respectively) are constants related to the relative quantum numbers $n_r, m_r$.[10] In writing the above energy for the relative motion [Eq. (9)] we have neglected the field independent term $-\gamma^2R_y^*/(n_r-1/2)^2$ (where $R_y^*=\mu e^4/2\varepsilon^2\hbar^2$ is the effective Rydberg), which does not give any contribution to the exciton trapping energy. In solving the exciton relative motion we assumed that the magnetic-field intensity is such that we are in the weak-field regime, i.e., $\hbar\omega_c^*<2R_y^*$ where $\omega_c^*=eB/\mu c$ is the cyclotron-resonance frequency. For GaAs this implies $B<5$ T.

For the sake of simplicity, instead of solving Eq. (6) to obtain $\gamma$, we used the results of Stébé and Moradi[23] and of Andreani and Pasquarello[24] to determine the zero-magnetic-field binding energy of excitons in GaAs/$Al_{0.3}Ga_{0.7}$As quantum wells.[25] We found that the gamma parameter only slightly influences the trapping energy and this as a coefficient in two smaller terms (diamagnetic and mass correction) in the exciton relative motion energy [see Eq. (9)]. For a complete description of the dependence of the $\gamma$ parameter with the quantum well width and also with an applied homogeneous magnetic field (which is negligible in the weak-field regime) we refer to Ref. 19.

The eigenenergy of the spin Hamiltonian for a magnetic field parallel to the z direction (for $d\ll a$ the in-plane magnetic field can be neglected) is straightforwardly calculated from Eq. (5c):

$$E^{m_z}(R)=\pm\frac{1}{2}\sqrt{\mu_B^2[(-1)^{m_z+1}g_{e,z}+g_{h,z}]^2B_z(R)^2+[c_x-(-1)^{m_z+1}c_y]^2}. \tag{11}$$

In the above energy, we neglected the $B(R)$-independent term, i.e., the $e$-$h$ exchange energy in the z direction $(-1)^{m_z+1}c_z/2$,[21] which does not contribute to the calculus of $E_T$. The spin-wave function is a linear combination $[|\mathcal{L}^{m_z}(\mathbf{R})\rangle=(|+\rangle\pm|-\rangle)/\sqrt{2}]$ of the exciton spin states $m_z$:

$$|\mathcal{L}^{m_z}(R)\rangle=\frac{||m_z|\rangle+(Q\pm\sqrt{1+Q^2})|-|m_z|\rangle}{\sqrt{2(1+Q^2\pm Q\sqrt{1+Q^2})}}, \tag{12}$$

where $Q=\mu_B[(-1)^{m_z+1}g_{e,z}+g_{h,z}]B_z(R)/[c_x-(-1)^{m_z+1}c_y]$.

We can now use all the results of the exciton relative motion, spin interaction, and well confinement [Eqs. (9), (11), and (6), respectively] to solve the exciton center-of-mass equation [see Eq. (5a)]. Now, the eigenenergies $E^r(\gamma,R,\nabla_R)$ and $E^{m_z}(R)$ act like an effective potential and an effective mass in the center-of-mass equation of motion:

$$\left\{-\frac{\hbar^2}{2M}\nabla_R\left\{1-\frac{e^2\mu}{\hbar^2Mc^2}\alpha_{m_r}^{n_r}\gamma^{-4}B_z(R)^2\right\}\nabla_R+\frac{e^2}{8\mu c^2}\beta_{m_r}^{n_r}\gamma^{-2}B_z(R)^2+\frac{e\hbar}{2\mu c}\xi B_z(R)m_r \pm\frac{1}{2}\sqrt{\mu_B^2[(-1)^{m_z+1}g_{e,z}+g_{h,z}]^2B_z(R)^2+[c_x-(-1)^{m_z+1}c_y]^2}-E\right\}\psi(R)=0. \tag{13}$$

Our magnetic field is parallel to the z direction and has $\varphi$ symmetry, i.e., $B_z(\mathbf{R})=B_z(R)$ [see Eq. (7)]. Then, we can use the cylindrical symmetry of our problem to write the exciton center-of-mass wave function as $\psi(\mathbf{R})=e^{-im_R\varphi}\psi(R)$, where $m_R$ is the quantum number for the angular momentum of the exciton center-of-mass motion. Inserting the above wave function in Eq. (13) and writing the $\nabla$ operator in cylindrical coordinates, Eq. (13) can be written as follows:

$$\left\{ -\frac{\hbar^2}{2}\frac{1}{R}\frac{d}{dR}\left[\frac{R}{M^{eff}(R)}\frac{d}{dR}\right] + V^{eff}(R) - E \right\} \psi(R) = 0, \tag{14}$$

where

$$M^{eff}(R) = \frac{M}{1 - \dfrac{e^2\mu}{\hbar^2 M c^2}\alpha_{m_r}^{n_r}\gamma^{-4}B_z(R)^2}, \tag{15a}$$

is the exciton effective mass, and

$$V^{eff}(R) = \frac{\hbar^2}{2}\frac{1}{M^{eff}(R)}\frac{m_R^2}{R^2} + \frac{e^2}{8\mu c^2}\beta_{m_r}^{n_r}\gamma^{-2}B_z(R)^2 + \frac{e\hbar}{2\mu c}\xi m_r B_z(R)$$

$$\pm\frac{1}{2}\sqrt{\mu_B^2[(-1)^{m_z+1}g_{e,z} + g_{h,z}]^2 B_z(R)^2 + [c_x - (-1)^{m_z+1}c_y]^2}, \tag{15b}$$

is the effective confinement potential of the exciton center-of-mass motion. In the above equation, the different terms correspond to the centrifugal, diamagnetic, orbital momentum, and spin contribution, respectively. The centrifugal term is related with the exciton effective mass and the angular momentum of the center-of-mass motion, which we found to give the smallest contribution to the effective potential. The magnetic-field squared dependence is present in the effective mass and in the diamagnetic term of the effective potential. Notice that all the direct contributions of the quantum well confinement is included through the $\gamma$ parameter, which only gives a small increase in the magnetic-field squared intensity. As occurs in the trapping of atoms, the two more important terms are the angular momentum and spin contributions. The first is only important for the excited states. The sign in the spin contribution is related to the spin quantum state $m_z = \pm 1, \pm 2$, which characterizes the spin Zeeman splitting.

## IV. NUMERICAL RESULTS AND DISCUSSION

We have calculated the trapping energy and wave function of excitons in a $GaAs/Al_{0.3}Ga_{0.7}As$ quantum well in a nonhomogeneous dipole type of magnetic field. The numerical solution of Eq. (14) was obtained by using a discretization technique. We use electron and heavy-hole $g$ factors that depend on the quantum well width $L$, but we neglect its magnetic-field dependence since only small magnetic-fields are considered.[26–28] We take advantage of the system symmetry to assume that $c_x = -c_y$.[27] The electron and heavy-hole mass, and the dieletric constant used in this paper are the same as in Refs. 23 and 24 ($m_e^*/m_0 = 0.067$, $m_h^*/m_0 = 0.34$, and $\varepsilon = 12.5$). The confinement energy level of the exciton in the quantum well does not directly enter into the trapping energy, but it enters indirectly through the $\gamma$ parameter, which depends on the confinement state of the exciton and on its relative motion state. As an example we took a ferromagnetic disk with radius $a = 2$ $\mu$m, which is placed a distance $d = 0.2$ $\mu$m above the quantum well.

The effective potential and effective mass for the exciton ground state is shown in Fig. 2 as a function of the radial coordinate $R$, for a quantum well width of $L = 90$ Å, for the situation in which a uniform applied field of (a) $B_a = 0.35$ T and (b) $B_a = -0.25$ T, is presented, where the strength of the disk magnetization is $B_0^D = 0.05$ T. The Zeeman effect can be seen in the effective potential by the shift in the corresponding spin states $m_z = \pm 1$ (dashed and dotted curves), as compared to the spinless state (solid curves). Notice that there is an interesting change of both sign and curvature in the effective potential associated to the spin states $m_z = \pm 1$, which can be observed by comparing the dotted curves ($m_z = +1$) with the dashed curves ($m_z = -1$) depicted in Fig. 2. This occurs due to the fact that the diamagnetic contribution to the effective potential [see Eq. (15b)] is usually smaller than the Zeeman contribution. Then, the lat-

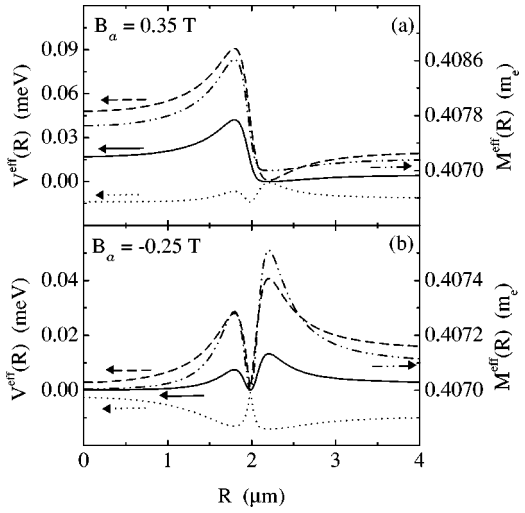


FIG. 2. Effective potential, $V^{eff}(R)$, for the exciton ground state, for the spinless situation $m_R = 0$ (solid), and respective effective mass, $M^{eff}(R)$, (dashed dotted), and $V^{eff}(R)$ for spin quantum states $m_z = +1$ (dotted), and $m_z = -1$ (dashed) of the magnetized disk, as a function of the radial coordinate $R$, for a homogeneous applied magnetic field of (a) $B_a = 0.35$ T and (b) $B_a = -0.25$ T, for $d/a = 0.1$ and $a = 2$ $\mu$m, for a strength of the disk magnetization of $B_0^D = 0.05$ T, and a quantum well width $L = 90$ Å.

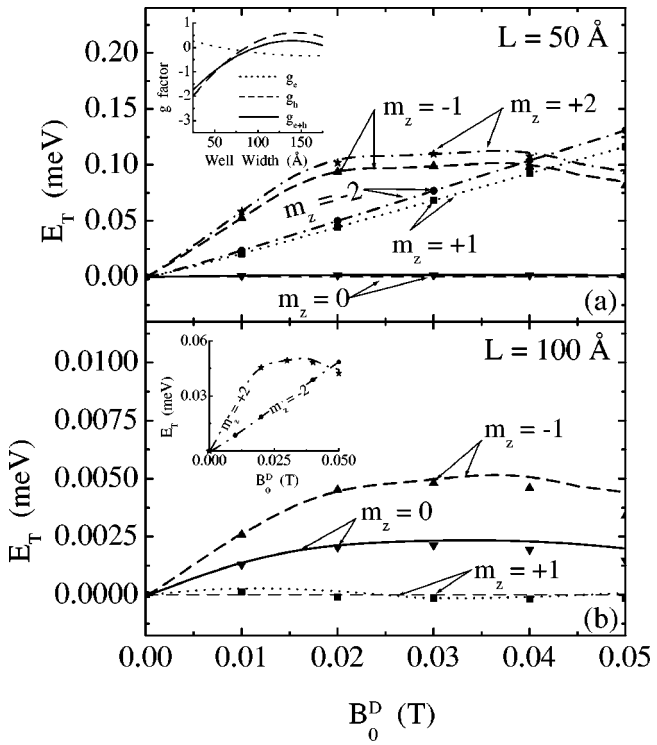


FIG. 3. Exciton trapping energy $E_T$ for $n_R=1$, $(n_r,m_r)=(1,0)$, as a function of the magnetization strength $B_0^D$, in the presence of an applied field $B_a=-0.25$ T and a quantum well width of (a) $L=50$ Å and (b) $L=100$ Å, with $m_R=0$ (curves) and $m_R=1$ (symbols), and for spin quantum numbers $m_z=0$ (solid curves and triangles down), $m_z=+1$ (dotted curves and squares), $m_z=-1$ (dashed curves and triangles up), $m_z=+2$ (short-dash curves and stars), and $m_z=-2$ (dashed-dotted curves and circles). In the inset of (a) the dependence of the $g$ factor on the quantum well width is shown.

ter dictates the behavior of the effective confinement potential, changing the confinement of the trapped exciton from a centered structure to a ringlike structure.

The quantum well confinement effects on the exciton motion are very important not because of the confinement itself, but due to the large dependence of the exciton $g$ factor on the

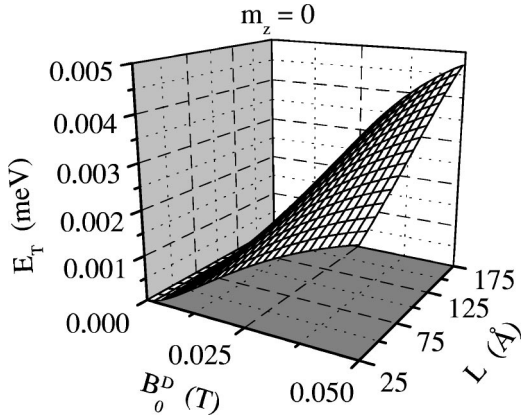


FIG. 4. Exciton trapping energy $E_T$ for the exciton ground state as a function of the strength of the disk magnetization $B_0^D$ and the quantum well width $L$, for the spinless exciton ($m_z=0$) and for an applied background field of $B_a=0.35$ T.

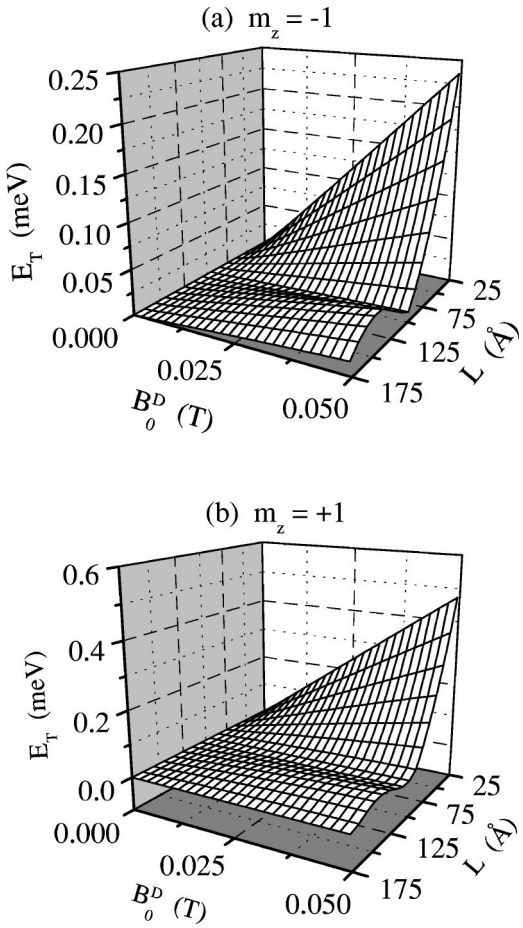


FIG. 5. The same as in Fig. 4 but now for spin quantum numbers (a) $m_z=-1$ and (b) $m_z=+1$.

quantum well width [see inset of Fig. 3(a)]. The exciton trapping energy dependence on the strength of the magnetization of the disk ($B_0^D$), for a homogeneous applied field of $B_a=-0.25$ T, for quantum well widths of $L=50$ Å and $L=100$ Å, is shown in Fig. 3(a) and Fig. 3(b), respectively. In both figures we showed the results for the case when the exciton center-of-mass quantum number is $n_R=1$ with $m_R=0$ (curves) and $m_R=1$ (symbols), and when the relative quantum numbers are $(n_r=1,\ m_r=0)$, for the ground-state level of the exciton well confinement, and for spin quantum number $m_z=0,\pm1$ (i.e., $\sigma^{\pm}$ polarized states), $\pm2$ (i.e., the dark excitons). The results for the dark exciton are only shown for reference. They are not optically active and they will not be further considered. Notice that the exciton $g$ factor increases the trapping energy as much as by a factor of 20 and that the behavior of the Zeeman splitting is strongly influenced by the nonhomogeneous magnetic field [compare the dashed and dotted curves in Fig. 3(a) and 3(b)]. Also notice that for large $B_0^D$, the trapping energy starts to decrease because the nonhomogeneous field created by $B_0^D$ can now be comparable to the homogeneous applied field $B_a$, which decreases the confinement region in the effective potential [see Fig. 2(b) and Fig. 1(b)]. The energy of the $m_R=1$ states [the centrifugal term in the effective potential of Eq. (15b)] are only slightly different from the energy of the corresponding nonexcited state.

The dependence of the exciton ground-state trapping en-

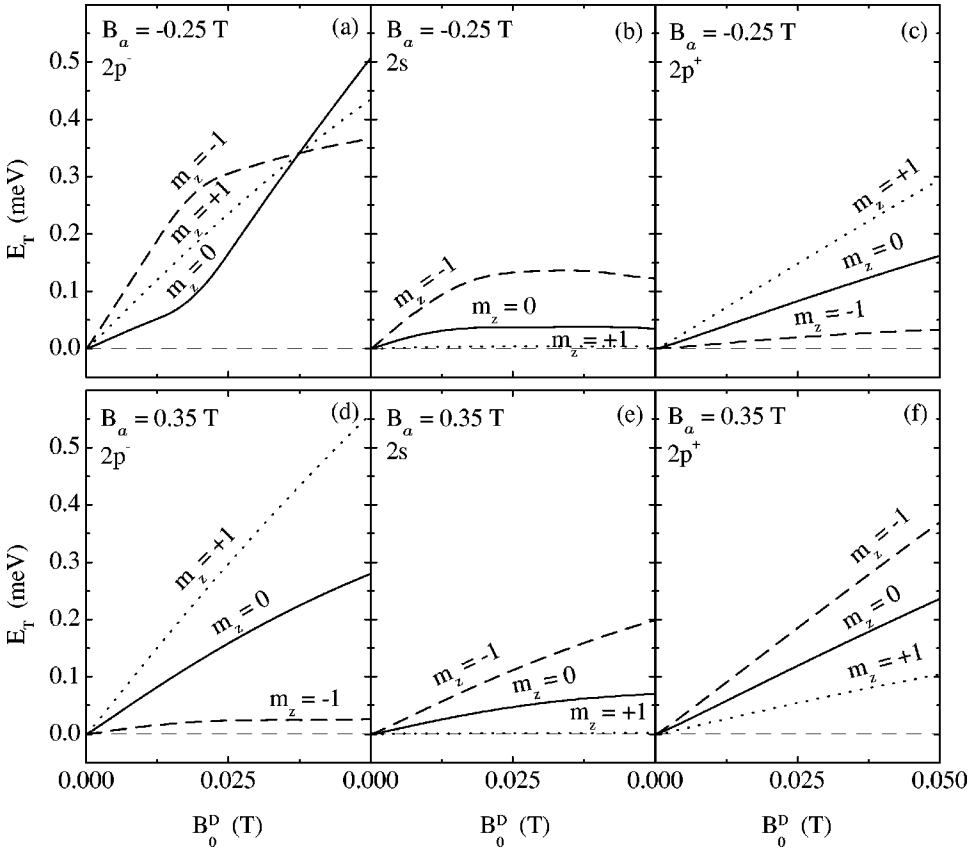


FIG. 6. Exciton trapping energy $E_T$ for $(n_R, m_R)=(1,0)$, $m_z=0$ (solid curves), $m_z=+1$ (dotted curves), $m_z=-1$ (dashed curves) as a function of $B_0^D$ in the presence of an applied field $B_a=-0.25$ T for relative quantum numbers (a) $(n_r, m_r)=(2,-1)$, (b) $(n_r, m_r)=(2,0)$, and (c) $(n_r, m_r)=(2,+1)$, and for $B_a=0.35$ T for $n_r=2$, and (d) $m_r=-1$, (e) $m_r=0$, and (f) $m_r=+1$. The quantum well width is $L=50$ Å.

ergy on the quantum well width and on the magnetization strength $B_0^D$ is shown in Figs. 4, 5(a), and 5(b), for the spin quantum numbers $m_z=0$, $-1$, and $+1$, respectively, and for an applied field $B_a=0.35$ T. For thin wells (widths smaller than approximately 60 Å) the exciton trapping energy is strongly sensitive to the nonhomogeneous magnetic field and to the size of the well. As the well width increases, the trapping energy becomes basically independent of the well confinement, and the magnetic field is only a small perturbation [see Figs. 5(a) and 5(b)]. There is a minimum in the exciton trapping energy when the quantum well width is near 100 Å, which is due to the fact that the $g$ factor is approximately equal to zero [see inset of Fig. 3(a)]. The spin Zeeman splitting, due to the nonhomogeneous magnetic field, does not follow the same behavior of shifting up and down the energy as occurs in the homogeneous field case [compare Figs. 4, 5(a), and 5(b)]. The $\sigma^-$ polarized state [Fig. 5(a)] is always shifted up as compared to the spinless situation (Fig. 4), but the $\sigma^+$ polarized state can be shifted down, but also up [see Fig. 5(b) or dotted curves in Figs. 3(a) and 3(b)], depending on the relation between the quantum well width (exciton $g$ factor) and the magnetization strength $B_0^D$. This is due to the change in the confinement region of the effective potential related with the $m_z=+1$ spin state, as previously described in our discussion of Fig. 2. It is quite remarkable that the exciton spin interaction with the nonhomogeneous magnetic field can be responsible for increases in the exciton trapping energy as large as a factor of 100, as compared to the spinless situation of Fig. 4. It is important to highlight that the considered magnetic fields and quantum well widths are in the range that are currently available experimentally.

The trapping energy of the exciton excited states as a function of the strength of the disk magnetization $B_0^D$ are shown in Fig. 6 for $(n_R=1,\ m_R=0)$ with relative quantum number $n_r=2$, for the first excited state of the exciton well confinement, for a quantum well width $L=50$ Å, for $B_a=-0.25$ T, with the following relative angular quantum numbers: (a) $m_r=-1$ , (b) $m_r=0$, and (c) $m_r=+1$, and for $B_a=-0.25$ T, for (d) $m_r=-1$ , (e) $m_r=0$, and (f) $m_r=+1$. The interaction of the exciton angular and spin momentum is responsible for several interesting effects, mainly in the case of negative $B_a$ where the Zeeman splitting exhibits different behavior for each angular quantum number of the relative motion. The trapping energy for a positive applied field always increases linearly with increasing nonhomogeneous magnetic-field intensity $B_0^D$, which is not the case for the results with negative $B_a$. The linear increase is due to the fact that the angular momentum term is the dominant term in the exciton Hamiltonian, and it has a linear dependence on the magnetic field. The decrease of the trapping energies in Figs. 6(a) and 6(b) can be explained by the competition between $B_a$ and $B_0^D$, as discussed previously in connection with Fig. 3.

The contour plot of the conditional probability to find the electron somewhere in the $xy$ plane for the case of the exci-

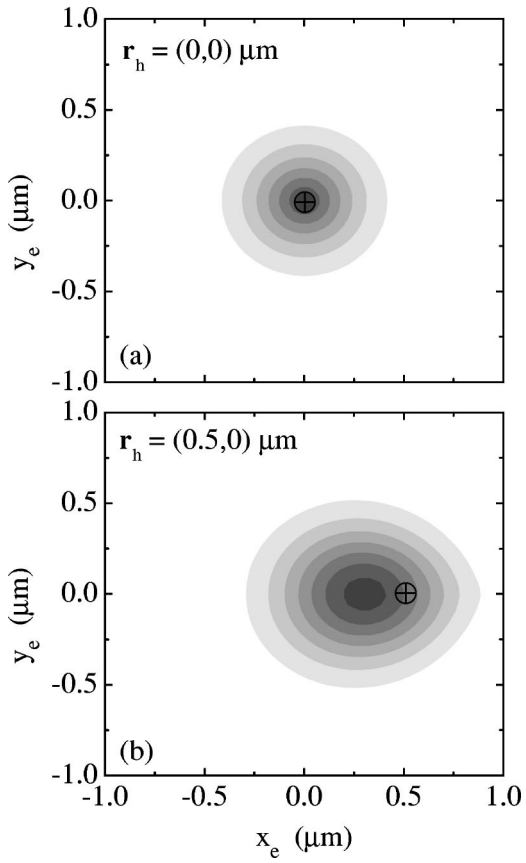


FIG. 7. Contour map of the electron conditional probability $|\psi(\mathbf{R})\Phi(\mathbf{r})|^2$ in the exciton ground state, for spin quantum number $m_z=-1$, quantum well width $L=90$ Å, magnetization strength $B_0^D=0.05$ T, and uniform applied field $B_a=-0.25$ T. We fixed the hole in position (a) $\mathbf{r}_h=(0,0)$ and (b) $\mathbf{r}_h=(0.5,0)$ $\mu$m.

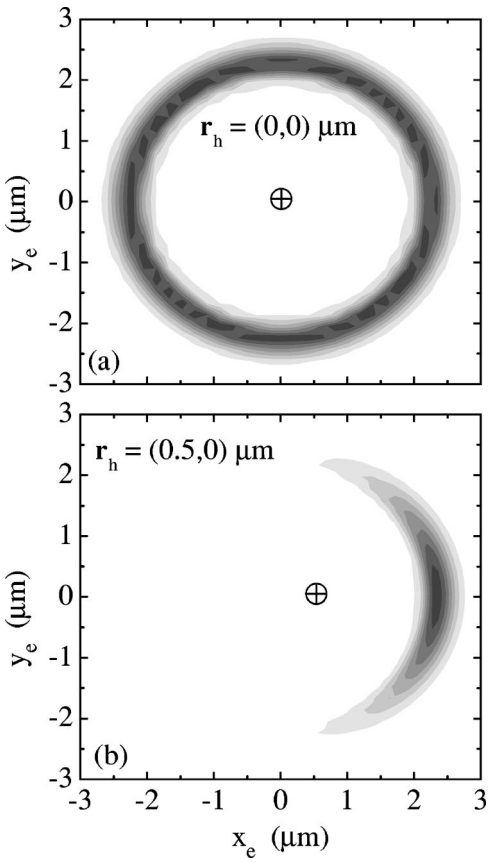


FIG. 8. The same as in Fig. 7 but now for spin quantum number $m_z=+1$.

ton ground state $|\psi(\mathbf{R})\Phi(\mathbf{r})|^2$, in the presence of an applied homogeneous magnetic field $B_a=-0.25$ T, is shown in Fig. 7 for the spin quantum number $m_z=-1$ and in Fig. 8 for $m_z=+1$. In both pictures, we considered a quantum well width $L=90$ Å and the strength of the disk magnetization was $B_0^D=0.05$ T. The hole (indicated by the symbol in the figures with a cross in the middle) is fixed in the position $\mathbf{r}_h=(0,0)$ in Figs. 7(a) and 8(a), and in $\mathbf{r}_h=(0.5,0)$ $\mu$m in Figs. 7(b) and 8(b). It can clearly be seen that the spin orientation changes the exciton confinement from a centered structure to a ringlike structure (compare Figs. 7 and 8). Also notice that the electron tries to follow the hole but this is partially worked against by the attraction to the minimum of the effective potential (see Fig. 2) in the case of a centered wave function (see Fig. 7). In the ringlike structure, the electron moves to the hole nearest position (see Fig. 8).

## V. CONCLUSIONS

The possibility of carrier trapping in a well-defined confinement region in a semiconductor heterostructure, opens the possibility of numerous studies for electronic phase transitions, confined exciton gases, and excitonic molecules.[6,7] The trapping of excitons in semiconductor systems of reduced dimensionality have also been proposed as a method of observing Bose-Einstein condensation of excitons.[9] The experimental efforts to observe exciton condensation in semiconductors were concentrated on the analysis of the PL line shape and the transport of excitons. Previous PL experiments (see, e.g., Ref. 11 and references therein) of the exciton trapping by using nonhomogeneous magnetic fields have shown that excitons are driven to regions of minimum field, but they could not detect the direct effect of the field gradient on the exciton motion. They concluded that the experimental conditions had to be improved by taking better samples that have larger exciton mobility, and a larger nonhomogeneous magnetic-field strength was necessary.

We have investigated the exciton trapping in a quantum well in the presence of a nonhomogeneous dipole type of magnetic field. The effects of the well confinement and of the exciton interaction with the nonhomogeneous magnetic field taking into account spin states, were analyzed and discussed. As compared to our previous results in which the spin of the exciton was not taken into account, we found a substantial increase of the trapping energy of the excitons by using nonhomogeneous magnetic fields. We also showed that the obtained energies, as well as the considered magnetic-field strength and well widths, are currently experimental obtainable.

Our results show that the trapping energy is strongly dependent on the quantum well width and shape of the nonhomogeneous magnetic-field profile, but that an increase in the magnetic-field intensity is not always related with a stronger confinement (as occurs in the uniform magnetic-field situation), as previously discussed in Sec. IV. Our main result is that the spin of the exciton is responsible for an increases in

the trapping energy, which can be as large as a factor of 100. This can be used to increase the experimental conditions by choosing a suitable set of parameters (quantum well width and magnetic-field profile) in order to maximize the exciton trapping. Furthermore, the spin interaction with the magnetic dipole type of profile can change the exciton spatial localization of a centered structure to a ringlike structure, increasing the energy level corresponding to the $m_z=+1$ spin state, which suggests that the two lines of the $\sigma^{\pm}$ polarized states will be very close in energy in the PL spectra, which may make it difficult for its identification. For the case of narrow wells, exciton localization due to quantum well width fluctuations will also be present. This effect was not considered in the present paper but should be easily distinguished experimentally with the present exciton trapping by nonhomogeneous magnetic field, by changing the strength of the magnetization of the magnetized disk.

Our results open up a new path for experiments on the confinement of excitons, which should reveal new kinds of exciton trapping and increase the knowledge about the exciton interaction with nonhomogeneous magnetic fields.

## ACKNOWLEDGMENTS

This research was supported by the Flemish Science Foundation (FWO-VI), the IUAP (Belgium), the ''Onderzoeksraad van de Universiteit Antwerpen,'' and by the Inter-University Micro-Electronics Center (IMEC, Leuven). J.A. K.F. was supported by the Brazilian Ministry of Culture and Education (MEC-CAPES) and F.M.P. was supported by the FWO-Vl. V.N.F. and G.A.F. would like to acknowledge the partial financial support received from CNPq, the Funding Agency of the Ceará State in Brazil (FUNCAP), and the Brazilian Ministry of Planning through FINEP.

*Permanent address: Departamento de Física, Universidade Federal do Ceará, Centro de Ciências Exatas, Campus do Pici, Caixa Postal 6030, 60455-760 Fortaleza, Ceará, Brazil. Electronic address: freire@uia.ua.ac.be

†Electronic address: peeters@uia.ua.ac.be

‡Permanent address: Semiconductor Physics Institute, Goštauto 11, 2600 Vilnius, Lithuania.

[1] C.E. Wieman, D.E. Pritchard, and D.J. Wineland, Rev. Mod. Phys. **71**, 253 (1999).

[2] E.A. Hinds, M.G. Boshier, and I.G. Hughes, Phys. Rev. Lett. **80**, 645 (1998).

[3] M.-O. Mewes, M.R. Andrews, N.J. van Druten, D.M. Kurn, D.S. Durfee, C.G. Townsend, and W. Ketterle, Phys. Rev. Lett. **77**, 988 (1996).

[4] V. Vuletic, T. Fischer, M. Praeger, T.W. Hänsch, and C. Zimmermann, Phys. Rev. Lett. **80**, 1634 (1998).

[5] D.P. Trauernicht, J.P. Wolfe, and A. Mysyrowicz, Phys. Rev. B **34**, 2561 (1986).

[6] L.V. Butov, A. Zrenner, G. Abstreiter, G. Böhm, and G. Weimann, Phys. Rev. Lett. **73**, 304 (1994).

[7] V. Negoita, D.W. Snoke, and K. Eberl, Appl. Phys. Lett. **75**, 2059 (1999).

[8] A.V. Korolev and M.A. Liberman, Phys. Rev. Lett. **72**, 270 (1994); D. Paquet, T.M. Rice, and K. Ueda, Phys. Rev. B **32**, 5208 (1985).

[9] L.V. Butov, A. Zrenner, M. Hagn, G. Abstreiter, G. Böhm, and G. Weimann, Surf. Sci. **361/362**, 243 (1996).

[10] J.A.K. Freire, A. Matulis, F.M. Peeters, V.N. Freire, and G.A. Farias, Phys. Rev. B **61**, 2895 (2000).

[11] F. Pulizzi, P.C.M. Christianen, J.C. Maan, T. Wojtowicz, G. Karczewski, and J. Kossut, Phys. Status Solidi A **178**, 33 (2000).

[12] For a recent review see: F.M. Peeters and J. De Boeck, in *Handbook of Nanostructured Materials and Nanotechnology*, edited by H.S. Nalwa (Academic Press, New York, 1999), Vol. 3, p. 345.

[13] M.A. McCord and D.D. Awschalom, Appl. Phys. Lett. **57**, 2153 (1990).

[14] K.M. Krishnan, Appl. Phys. Lett. **61**, 2365 (1992).

[15] S.J. Bending, K. von Klitzing, and K. Ploog, Phys. Rev. Lett. **65**, 1060 (1990).

[16] M.L. Leadbeater, C.L. Foden, T.M. Burke, J.H. Burroughes, M.P. Grimshaw, D.A. Ritchie, L.L. Wang, and M. Pepper, J. Phys.: Condens. Matter **7**, L307 (1995).

[17] S.V. Dubonos, A.K. Geim, K.S. Novoselov, J.G.S. Lok, J.C. Maan, and M. Henini, Physica E (Amsterdam) **6**, 746 (2000).

[18] A.K. Geim, I.V. Grigorieva, S.V. Dubonos, J.G.S. Lok, J.C. Maan, A.E. Lindelof, and F.M. Peeters, Nature (London) **390**, 259 (1997).

[19] B.-H. Wei, Y. Liu, S.-W. Gu, and K.-W. Yu, Phys. Rev. B **46**, 4269 (1992).

[20] S.V. Branis and K.K. Bajaj, Phys. Rev. B **45**, 6271 (1992).

[21] H.W. van Kesteren, E.C. Cosman, W.A.J.A. van der Poel, and C.T. Foxon, Phys. Rev. B **41**, 5283 (1990).

[22] M. Born and K. Huang, *Dynamical Theory of Crystal Lattices* (Clarendon Press, Oxford, 1968).

[23] B. Stébé and A. Moradi, Phys. Rev. B **61**, 2888 (2000).

[24] L.C. Andreani and A. Pasquarello, Phys. Rev. B **42**, 8928 (1990).

[25] For the calculus of $\gamma$, we compare the energy of the zero field term in the exciton relative motion $[-\gamma^2 R_y^*/(n_r-1/2)^2]$ with the corresponding data in the literature for the exciton binding energy, i.e., $\gamma^2=E_b^{lit.}/[R_y^*/(n_r-1/2)^2]$.

[26] M.J. Snelling, E. Blackwood, C.J. McDonagh, R.T. Harley, and C.T.B. Foxon, Phys. Rev. B **45**, 3922 (1992).

[27] E. Blackwood, M.J. Snelling, R.T. Harley, S.R. Andrews, and C.T.B. Foxon, Phys. Rev. B **50**, 14 246 (1994).

[28] R.T. Harley and M.J. Snelling, Phys. Rev. B **53**, 9561 (1996).